

Quantitation of a *Glyptapanteles indiensis* polydnavirus gene expressed in parasitized host, *Lymantria dispar*, by real-time quantitative RT-PCR

Y.P. Chen^{a,1}, J.A. Higgins^b, D.E. Gundersen-Rindal^{a,*}

^a US Department of Agriculture (USDA)–Agricultural Research Service (ARS), Insect Biocontrol Laboratory, Room 214, Building 011A BARC West, Beltsville, MD 20705, USA

^b US Department of Agriculture (USDA)–Agricultural Research Service (ARS), Environmental Microbial Safety Laboratory, Beltsville, MD 20705, USA

Received 7 May 2003; received in revised form 18 August 2003; accepted 20 August 2003

Abstract

Glyptapanteles indiensis is a polydnavirus-carrying wasp that parasitizes early instar gypsy moth larvae. During oviposition, the wasp injects calyx fluid containing polydnavirus along with its eggs into the host. Within the host, expression of polydnavirus genes triggers a set of changes in host physiology, which are of critical importance for the survival of the wasp. In the present study, a *G. indiensis* polydnavirus (GiPDV) gene, represented by cDNA clone GiPDV 1.1, was selected for expression analysis in the parasitized host. The GiPDV 1.1 gene transcript was detected in host hemolymph 30 min post-parasitization (pp) and continued to be detected for six days. The level of GiPDV 1.1 expression varied in different host tissues and expression in the brain was lower than in the hemolymph. The findings suggest that GiPDV 1.1 could be involved in early protection of parasitoid eggs from host cellular encapsulation. The temporal and spatial variations in PDV gene expression in different host tissues post-parasitization affirm their specific host regulation mechanism.

© 2003 Elsevier B.V. All rights reserved.

Keywords: *Glyptapanteles indiensis*; *Lymantria dispar*; Polydnavirus; Parasitization; Gene expression; Real-time quantitative RT-PCR

1. Introduction

Polydnaviruses (PDVs) are a group of symbiotic viruses carried by parasitic wasps in the families Ichneumonidae and Braconidae. PDVs are characterized by their segmented double-stranded DNA genomes, their transmission mode, and their roles in host regulation. The PDV genome is integrated in the wasp genome as provirus and virions replicate only in specialized cells of the ovaries. During oviposition, virus is injected along with parasite eggs into the host larva. Within host tissues, PDVs do not replicate, but host-specific viral genes are expressed. The expression of viral genes in the parasitized host triggers a set of changes in host phys-

iology, which are of critical importance for the survival of the endoparasitic wasp. One profound PDV-induced effect is an alteration of host immune response, which prevents parasitic eggs from undergoing cellular encapsulation. The parasitic eggs are encapsulated by the host's cellular immune system when co-injected with UV inactivated virus or injected without their associated PDV. However, the eggs are not encapsulated when co-injected with purified PDV (Edson et al., 1981; Strand and Wong, 1991; Strand and Noda, 1991). Other significant physiological effects, such as developmental arrest, growth inhibition, and susceptibility to disease infection are also reported to be associated with certain PDV genes (reviewed in Lawrence and Lanzrein, 1993; Stoltz, 1993; Lavine and Beckage, 1995). Clearly, characterization of gene expression in the parasitized host is important for understanding the mechanism of GiPDV in the suppression of the host immune system.

The braconid *Glyptapanteles indiensis* parasitizes early instar gypsy moth (*Lymantria dispar*) larvae. *G. indiensis* polydnavirus (GiPDV) suppresses the host immune

* Corresponding author. Tel.: +1-301-504-6692; fax: +1-301-504-5104.

E-mail address: gundersd@ba.ars.usda.gov (D.E. Gundersen-Rindal).

¹ Present address: US Department of Agriculture (USDA)–Agricultural Research Service (ARS), Bee Research Laboratory, Beltsville, MD 20705, USA.

response, preventing encapsulation of parasitoid eggs, which appears to be a prerequisite for successful parasitization. Previous genomic organization studies (Chen and Gundersen-Rindal, 2003) indicated the GiPDV genome was comprised of at least 13 different dsDNA segments, ranging in size from 11 kb to more than 30 kb. The DNA segments were heterogeneous in size and molar ratio. Physical mapping indicated that isolated cDNA clones containing GiPDV-specific sequences expressed in the parasitized host were present on more than one genomic DNA segment. These results suggested the existence of homologous sequences among GiPDV DNA segments as reported for other PDVs (Xu and Stoltz, 1993; Cui and Webb, 1997). Genome segmentation, hypermolar ratio segments and segment nesting were believed to have functional significance, evolved to increase the copy number of essential genes or to increase levels of functional gene expression in the absence of virus replication (Xu and Stoltz, 1993; Cui and Webb, 1997). In correspondence with this assumption, highly expressed viral genes in the ichneumonid *Campoletis sonorensis* PDV were reported to be associated with nested DNA segments (Webb, 1998). The appearance of isolated cDNA homologs on multiple DNA segments suggested these genes may be highly expressed in the parasitized host. Analysis of GiPDV gene expression in the parasitized host would be necessary to confirm this.

A number of methods are available currently for studying gene expression, including Northern blot, in situ hybridization, ribonuclease protection assay, and quantitative reverse transcription-polymerase chain reaction (RT-PCR). Of these, quantitative RT-PCR has proven to be the most powerful tool for measurement of mRNA transcripts expressed at very low levels. Originally, quantitative competitive RT-PCR (qPCR) was developed and shown to be an accurate method for quantification of mRNA expression (Raeymaekers, 1995). This method requires cloning procedures for the construction of a internal standard (competitor) and co-amplification of a known amount of competitor with an unknown amount of sample in the same tube. Although qPCR assay provides a strategy for accurate quantitation, this method is time consuming and technically sophisticated. Real-time quantitative RT-PCR is a recently developed method for quantitative analysis of gene expression. This technique uses the 5′–3′ nucleolytic activity of *Taq* DNA polymerase to cleave a dual fluorescently-labeled hybridization probe during the extension phase of PCR; the fluorescence released after cleavage is used to quantify the target-specific PCR product during amplification (real-time detection). Results are expressed in terms of the threshold cycle number or C_T , the number of cycles needed to generate a fluorescent signal above a predefined threshold (usually 10 times the standard deviation of the background fluorescence intensity which is measured between cycle 3 and 15). The C_T value reflects the relative quantity of the original mRNA. Greater amounts of initial transcripts usually result in a lower C_T values. Real-time quantitative

RT-PCR combines PCR amplification and product detection in one step without post-PCR analysis of product by gel electrophoresis, and provides a good basis for mRNA quantitation. In the present study, one of our previously isolated cDNA clones, designated GiPDV 1.1 (Chen and Gundersen-Rindal, 2003), was selected for gene expression analysis. By using real-time TaqMan quantitative RT-PCR method, GiPDV 1.1 gene expression in parasitized *L. dispar* tissues at different times post-parasitization (pp), was examined. In order to normalize gene expression levels, the expression of a *L. dispar* housekeeping gene, β -actin, was also monitored. This is the first report of real-time quantitative RT-PCR employed for analysis of PDV gene expression.

2. Materials and methods

2.1. Insects

Both *G. indiensis* and *L. dispar* were reared at 26°C, 50% RH, and a 16L:8D photo period (Bell et al., 1981). *L. dispar* larvae were mass reared in plastic cups with species-specific artificial diets (Bell et al., 1981). *G. indiensis* was reared from *L. dispar* larva as described (Chen and Gundersen-Rindal, 2003). Second-instar larva were parasitized by exposing individual larva to mated *G. indiensis* females within a 35 mm × 10 mm petri dish. After a single oviposition was observed, the parasitized larva was removed to avoid superparasitization. Times pp were recorded from initiation of parasitization.

2.2. RNA isolation

For analysis of GiPDV-1.1 gene expression in different host tissues, hemolymph was drawn from parasitized larvae at a series of time periods pp. (30 minutes, 2, 4, 6, 8, and 10 days) with a capillary tube through an opening made by cutting off a hindleg. The parasitization of 20 larvae usually took 30 min and parasitized larvae subjected to RNA extraction immediately pp were designated as 30 min pp. After hemolymph collection, the larvae were dissected in a PBS solution under the microscope for collection of brain tissue. In order to prevent possible contamination with hemolymph, brain tissue was rinsed with PBS solution three times prior to RNA extraction.

Immediately after tissue collection, total RNA was extracted from each tissue using TRIzol reagent according to the manufacturer's instructions (Invitrogen). RNA samples were resuspended in DEPC-treated water in the presence of ribonuclease inhibitor (Invitrogen). As controls, RNA samples were also collected from nonparasitized larvae. The quality of RNA samples was confirmed by formaldehyde gel electrophoresis.

All RNA samples were treated with DNase I (Invitrogen) prior to real-time quantitative RT-PCR. The absence of contaminating genomic DNA in the RNA samples was verified by running PCR directly without reverse transcription.

2.3. GiPDV 1.1 sequence and oligonucleotides for real-time RT-PCR

GiPDV 1.1 nucleotide sequences (GenBank accession number AF414845) and predicted amino acid sequences were analyzed with CBS Prediction Server.

Primers and probes for GiPDV-1.1 and *L. dispar* β -actin (GenBank accession number AF182715) were designed using primer expression version 1.0 (PE Applied Biosystems). Primers and TaqMan probes for both GiPDV 1.1 and β -actin genes were designed to amplify less than 220 bp PCR products. Probe sequences were selected to obtain a T_m approximately 10 °C higher than the matching primer pairs. The GiPDV 1.1 primers were GiPDV 1.1-F (5'-GCACCATATTGACGTTGCTCA-3') and GiPDV 1.1-R (5'-CCACCTTTACGACCGATCCA-3'). GiPDV 1.1 TaqMan probe was GiPDV1.1-P (FAM-AATACCGCGATCGA-AGCCTTAACGGT-TAMRA). Primers and probe for GiPDV 1.1 amplify a 210 bp fragment. The β -actin primers were β -actin-F (5'-GGGACAGAAGGACTCGTACG-3') and β -actin-R (5'-GCCTTAGGGTTGAGAGGAGC-3'). The β -actin TaqMan probe was β -actin-P (FAM-TTCTACA-ATGAAGTGGTGTGCGCC-TAMRA). Primers and probe for β -actin amplify a 201 bp fragment. Primers and probes used in the real-time quantitative RT-PCR were purchased from Perkin-Elmer Applied Biosystems.

2.4. Real-time quantitative RT-PCR

GiPDV-1.1 gene expression in different host tissues and at different times pp were quantified with real-time quantitative RT-PCR and performed on a Stratagene Mx4000TM multiplex quantitative PCR system using TaqMan chemistry for thermal cycling and real-time fluorescence measurements. The GiPDV 1.1 probe was labeled with a reporter dye (FAM, fluorescent dye carboxyfluorescein) at the 5' end and a quencher dye (TAMRA, *N,N,N',N'*-tetramethyl-6-carboxyrhodamine) at the 3' end. During the PCR extension phase, the probe hybridized with the cDNA region was degraded by the 5'-exonuclease activity of *Taq* polymerase, separating the quencher from the reporter. This resulted in a subsequent increase in the level of fluorescence emission of the reporter dye in the reaction mixture.

Real-time RT-PCR was carried out using the one-step access RT-PCR system (Promega). The reaction mixture (50 μ l) consisted of the following: 1 \times AMV/Tfl reaction buffer, 200 μ M each dNTP, 2 mM MgSO₄, 0.5 μ M each forward and reverse primers, 0.4 μ M TaqMan probe, 0.1 unit AMV reverse transcriptase, 0.1 unit Tfl DNA polymerase, and 500 ng of total RNA. The reaction was performed under the following conditions: one cycle at 48 °C for 45 min; 95 °C for 2 min; 40 cycles at 95 °C for 30 s, 50 °C for 1 min, and 68 °C for 2 min. Each RT-PCR amplification was repeated in triplicate, with each replicate performed on a different day.

Real-time quantitative RT-PCR for the *L. dispar* β -actin gene was also performed on each sample as an internal control for equivalence of template. Amplification of the β -actin gene was performed under the same conditions as described.

2.5. Detection and quantitation

Fluorescence values were measured and amplification plots were generated in real-time by the Mx4000TM system software. Amplification results were expressed as the C_T value, which represents the cycle at which fluorescence rose above a predefined threshold value. In this study, the predefined threshold values were based on a 10 \times standard deviation of the raw fluorescence detected from cycles 3–5. Agarose gel electrophoresis analysis was also performed to verify that the amplified product corresponded to the size predicted for gene-specific product.

Quantitative analysis of GiPDV 1.1 expression was done using the comparative $C_T(\Delta C_T)$ method since synthetic RNA corresponding to the GiPDV 1.1 gene was not available. The comparative C_T method is similar to the standard curve method, except it uses arithmetic formulas to achieve the same result for relative quantitation. For the comparative C_T method to be successful, amplification efficiencies of both the GiPDV 1.1 and β -actin RT-PCRs should be similar. To confirm this, a validation experiment was performed. Seven 5-fold serial dilutions (500, 100, 20, 4, 0.8, 0.16, and 0.032 ng) of total RNA sample were used for the GiPDV 1.1 and β -actin RT-PCR amplification. The relative expression of GiPDV 1.1 was normalized to an endogenous reference (β -actin gene) by subtracting the C_T value of β -actin from the C_T value of GiPDV 1.1 for each dilution of RNA and expressed as $\Delta C_T(\Delta C_T = C_{T, \text{GiPDV1.1}} - C_{T, \beta\text{-actin}})$. If the plot of log input amount of total RNA versus ΔC_T had a slope less than 0.1, the amplification efficiencies of the GiPDV 1.1 and β -actin genes were approximately equal, and the comparative C_T method could be used. The expression of GiPDV 1.1 relative to a calibrator was described as $2^{-\Delta \Delta C_T}$, where $\Delta \Delta C_T = \Delta C_{T(\text{sample})} - \Delta C_{T(\text{calibrator})}$; the sample that represented the lowest detectable level of GiPDV 1.1 expression was chosen as a calibrator.

2.6. Statistical analysis

Statistix7 statistical software (Analytic Software, Tallahassee, FL, USA) was used for statistical analysis. The results, in terms of C_T values are shown as mean \pm S.D. for triplicate RT-PCR reactions. Statistically significant differences of β -actin gene expression between different times pp and between different host tissues were calculated by a Student's *t*-test for unpaired data. The equations for relative standard curves and relative efficiency plots were calculated by linear regression analysis.

3. Results

3.1. Nucleotide sequence and deduced translated amino acid sequence of GiPDV 1.1

As reported previously, analysis of GiPDV 1.1 sequence identified one large open reading frame of 1275 nucleotides encoding 425 amino acids (Fig. 1). The ORF was flanked by 24 bp of 5'-UTR and 82 bp of 3'-UTR, followed by the poly-A tail. A BLAST (Altschul et al., 1990) search indicated no significant nucleotide or amino acid sequence homologies to known sequences in GenBank. The N-terminal of the predicted GiPDV 1.1 protein sequence had a 21 hydrophobic amino acid signal peptide and a cleavage site between amino acid position 21 and 22. The predicted amino sequence of GiPDV 1.1 had a calculated molecular mass of 36 kDa after cleavage of the putative signal peptide, six potential N-linked glycosylation sites (NVSA, 119–122; NQTQ, 159–162; NGTE, 223–226; NLSD, 230–233; NYTS, 255–258; NKTQ, 265–268), and five potential protein kinase C phosphorylation sites (SNR, 170–172; SNK, 211–213; SNK, 264–266; TER, 225–227; TNR, 260–262). A polyadenylation signal (AAUAAA) was found at nucleotide position 1064, 15 bp upstream of the poly-A tail.

3.2. Regression of threshold cycle (C_T) values on the amount of input RNA

Preliminary experiments were conducted to determine the effects of concentration of primer and $MgSO_4$ on efficiency of amplification, using the conventional RT-PCR method. Results indicated that 2 mM $MgSO_4$ and 0.5 μM of each primer gave optimal amplification. Also, prior to real-time RT-PCR analysis, control experiments without reverse transcription were conducted to confirm that all RNA samples were free of genomic DNA contamination.

To determine the linear dynamic range of template concentration, standard curves for GiPDV 1.1 and β -actin genes were plotted as log input RNA versus corresponding threshold cycle (C_T). As shown in Fig. 2, a strong linear relationship was observed between the amount of input RNA and the C_T values over seven log serial dilutions, and similar amplification efficiencies were observed for both GiPDV 1.1 and β -actin genes. The GiPDV 1.1-specific reactions showed a linear relationship between C_T value of 15.78 ± 0.60 (log 500 ng of total RNA) and C_T value of 31.60 ± 0.07 (log 32 pg of total RNA). The β -actin-specific reactions also showed a linear relationship between C_T value of 14.97 ± 0.63 (log 500 ng of total RNA) and C_T value of 28.75 ± 0.06 (log 32 pg of total RNA). Regression analysis of the C_T value generated by the log serial dilutions produced a R^2 value of 0.98 and 0.95 for GiPDV 1.1 and β -actin genes, respectively. The results suggested use of a template concentration within this range resulted in linear progression of the amplification.

3.3. Validation of amplification efficiency for GiPDV1.0 and β -actin RT-PCR

In order to use the comparative C_T method for quantitative analysis, the efficiencies of GiPDV1.1 and β -actin amplification in the real-time RT-PCR were evaluated. Relative efficiencies of GiPDV 1.1 and β -actin amplification were plotted as $\Delta C_T = (C_{T(GiPDV1.1)} - C_{T(\beta\text{-actin})})$ versus the log of the corresponding amounts of input RNA. As shown in Fig. 3, the plot of log input RNA versus ΔC_T had a slope less than 0.1 (slope = 0.013), indicating that efficiencies of GiPDV 1.1 and β -actin were approximately equal. Therefore, the comparative C_T method for the relative quantification of GiPDV1.1 gene expression was applicable.

The quality of all tested samples in the study was verified by RT-PCR detection of the β -actin gene. The β -actin gene expression remained constant during the whole experimental period with C_T values ranging from 15.07 to 15.69 (Table 1). No significant differences of β -actin gene expression were observed among the samples ($\rho = 0.001$).

3.4. Relative quantitation of GiPDV 1.1 gene expression in parasitized host

GiPDV1.1 expression levels were normalized to the endogenous reference β -actin. Brain sample collected 6 days pp (B-6d) was chosen as a calibrator, because it represented the lowest detectable level of GiPDV 1.1 expression. The GiPDV 1.1 expression values of all other samples were analyzed relative to that of B-6d. As summarized (Table 1), GiPDV 1.1 expression levels changed significantly, varying from 1.2- to 191-fold. The highest relative expression was observed in hemolymph 30 min pp. Relative levels of GiPDV 1.1 gene expression descended for hemolymph-30 min > hemolymph-2d > hemolymph-4d > brain-4d > hemolymph-6d > brain-6d.

GiPDV 1.1 transcript could be detected in hemolymph of parasitized host larvae 30 min pp and expression remained active for 6 days pp. However, the level of GiPDV 1.1 expression declined significantly in hemolymph 6 days pp ($\rho = 0.013$). No detectable GiPDV1.1 expression was observed in hemolymph 8 days pp and thereafter (data not shown). No RT-PCR product was detected from the hemolymph of non-parasitized host larvae. A representative amplification plot of GiPDV 1.1 expression in hemolymph of parasitized *L. dispar* larvae is shown in Fig. 4.

The relative level of GiPDV 1.1 expression in the brain of parasitized hosts was lower than in the hemolymph. The timing of GiPDV 1.1 expression in the brain of parasitized hosts was also slower than that in the hemolymph. No GiPDV 1.1 amplification product was detected in the brains of parasitized larvae at times 30 min and 2 days pp. However, signal from GiPDV 1.1 expression was detected in the brain of parasitized larvae 4 and 6 days pp. The brain sample 6 days pp had the highest C_T and ΔC_T values, and therefore it represented the lowest detectable

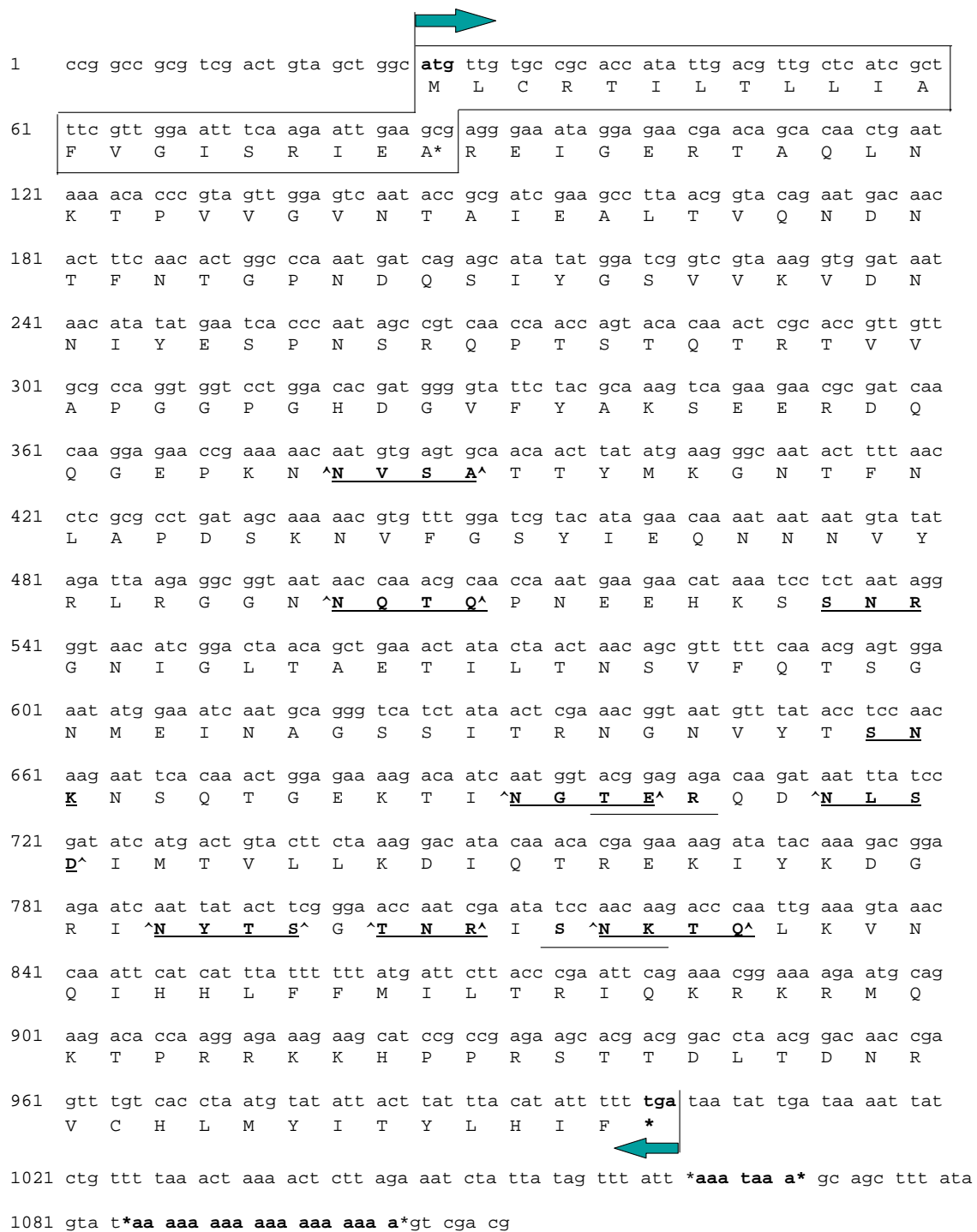


Fig. 1. Nucleotide sequence and deduced translated amino acid sequence of GiPDV 1.1. Start and stop codons are bold and indicated by an arrow. The predicted hydrophobic leader sequence is boxed. The cleavage site between position 21 and 22 is indicated by an asterisk. Potential N-linked glycosylation sites are shown in bold, underlined, and indicated by carets. Potential protein kinase C phosphorylation sites are shown in bold and underlined. Potential polyadenylation signal and poly-A tail are shown in bold and flanked by asterisks.

level of GiPDV 1.1 expression. No expression was detected on day 8 pp and thereafter. No RT-PCR product was amplified from the brain of nonparasitized host larvae. A representative amplification plot of GiPDV 1.1 expression in brain of parasitized *L. dispar* larvae is shown in Fig. 5.

4. Discussion

In the present study, the real-time TaqMan RT-PCR technique was used to detect GiPDV 1.1 gene expression, and the comparative C_T method was used to quantify relative

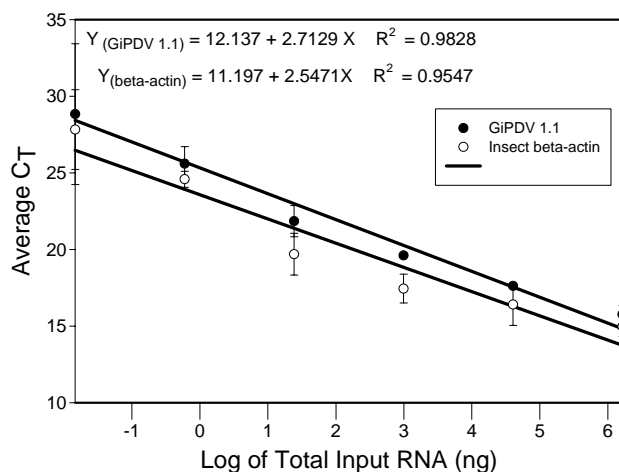


Fig. 2. Regression of threshold cycle (C_T) values on the amount of input RNA. The range of input RNA was from 500 ng to 32 pg. Each data point represents the mean of triplicate reactions: (●) regression of GiPDV 1.1-specific product and (○) regression of β -actin-specific product.

GiPDV 1.1 gene expression in *L. dispar* larvae parasitized by *G. indiensis*. The accuracy and validity of the detection and quantitative method were confirmed by demonstration of stable expression of β -actin, and equivalent amplification efficiencies of GiPDV 1.1 and β -actin genes in samples. Compared with other previously described PCR-based assays, real-time RT-PCR presents several advantages. First, real-time RT-PCR gives a more accurate and reproducible quantitation because it is based on the C_T value in the early cycles of a PCR reaction rather than end-point PCR measurement. Second, real-time RT-PCR does not require the design and cloning of an internal competitor. Third, real-time RT-PCR enables one to run multiple reactions for several genes in the same reaction plate. Finally, real-time RT-PCR does not require post-reaction manipulation, saving time and

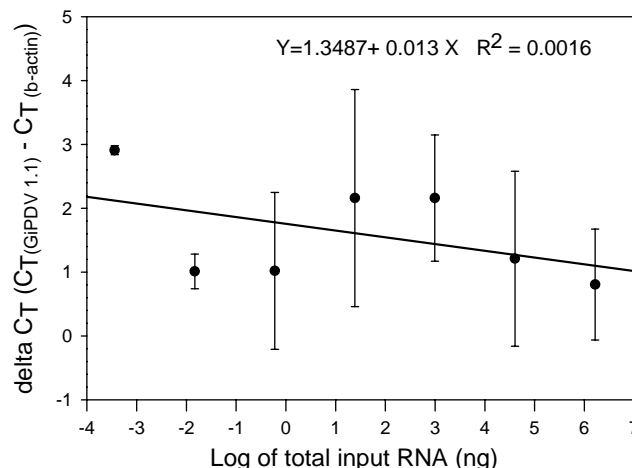


Fig. 3. Validation of amplification efficiency for GiPDV1.1 and β -actin RT-PCR. The difference of GiPDV 1.1 C_T value and β -actin C_T value ($\Delta C_T = C_{T(\text{GiPDV1.1})} - C_{T(\beta\text{-actin})}$) was plotted vs. the log of the total RNA concentration. The plot of log total RNA input versus ΔC_T has a slope less than 0.1, indicating that the efficiencies of the two amplicons were approximately equal. Therefore, the $\Delta \Delta C_T$ calculation for the relative quantitation of GiPDV 1.1 gene expression was applicable.

reducing the risk of PCR contamination. One disadvantage of the real-time RT-PCR method is that quantification is relative if a synthetic target RNA is not available, compared with the absolute quantification values obtained using the competitive RT-PCR method.

In order to characterize the functional role of GiPDV1.1 in the parasitized host, temporal GiPDV 1.1 gene expression in hemolymph and brain of the parasitized host was investigated. Remarkably, GiPDV1.1 transcripts could be detected in host hemolymph less than one hour pp and continued to be detected for 6 days. Gene expression in the hemolymph 30 min pp was the highest among all tested samples. The

Table 1

Relative quantification of the GiPDV 1.1 gene expression in parasitized host by real-time quantitative RT-PCR using the comparative C_T method

Tissues	GiPDV 1.1 (average C_T)	β -Actin (average C_T)	ΔC_T^a ($C_{T(\text{GiPDV1.1})} - C_{T(\beta\text{-actin})}$)	$\Delta \Delta C_T^b$ ($\Delta C_T - \Delta C_{T(\text{calibrator})}$)	$2^{-\Delta \Delta C_T^c}$
Hemolymph					
30 min	15.57 \pm 0.11	15.07 \pm 0.38	0.50 \pm 0.40	-7.58 \pm 0.40	191 (145–252)
2 days	16.19 \pm 0.23	15.50 \pm 0.65	0.69 \pm 0.68	-7.39 \pm 0.68	167 (105–268)
4 days	16.15 \pm 0.45	15.40 \pm 0.77	0.75 \pm 0.89	-7.33 \pm 0.89	161 (87–298)
6 days	23.29 \pm 0.88	15.42 \pm 0.64	7.87 \pm 1.08	-0.21 \pm 1.08	1.2 (0.5–2)
Brain					
30 min	0	15.69 \pm 1.00			
2 days	0	15.38 \pm 0.73			
4 days	17.91 \pm 0.62	15.45 \pm 0.76	2.42 \pm 0.98	-5.66 \pm 0.98	50 (26–100)
6 days*	23.70 \pm 0.40	15.62 \pm 0.76	8.08 \pm 0.85	0.00 \pm 0.85	1 (0.5–2)

^a The ΔC_T value is determined by subtracting the average C_T value of β -actin from the average C_T value of GiPDV 1.1. The standard deviation of the difference is calculated from the standard deviation of the GiPDV 1.1 and β -actin values using the formula: $S = \sqrt{S_{(\text{GiPDV1.1})}^2 + S_{(\beta\text{-actin})}^2}$.

^b The $\Delta \Delta C_T$ value is determined by subtracting the ΔC_T value of calibrator from the ΔC_T value of particular sample. Brain sample 6 days post-parasitization was chosen as a calibrator as it represented the minimum level of GiPDV 1.1 expression demonstrated by the highest C_T and ΔC_T values. Calibrator is indicated by an asterisk. The standard deviation of $\Delta \Delta C_T$ is the same as the standard deviation of the ΔC_T value.

^c The $\Delta \Delta C_T$ expression of GiPDV 1.1 relative to a calibrator was described as $2^{-\Delta \Delta C_T}$. The range for $2^{-\Delta \Delta C_T}$ value is based on $\Delta \Delta C_T + S$ and $\Delta \Delta C_T - S$, where S is the standard deviation of the $\Delta \Delta C_T$ value.

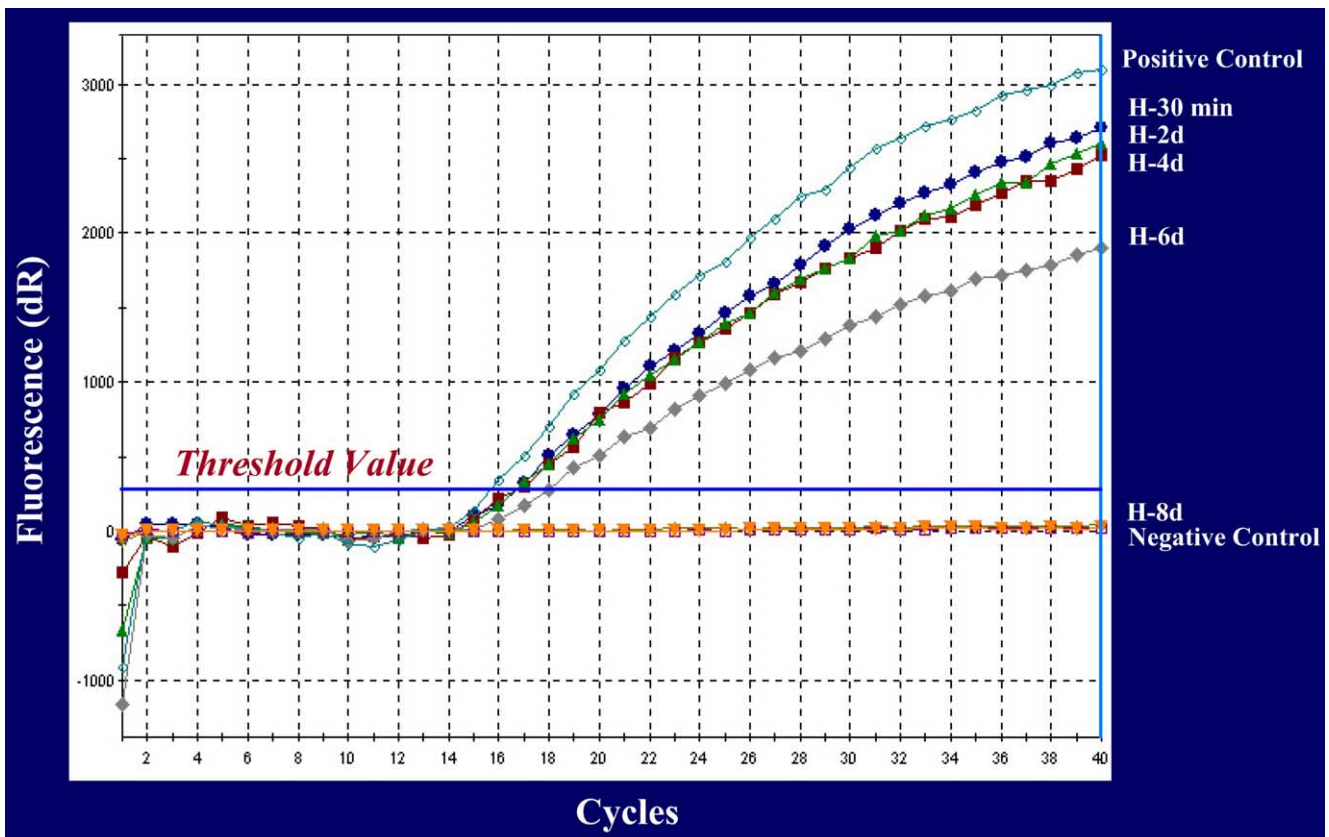


Fig. 4. Representative RT-PCR amplification plot of GiPDV 1.1 expression in hemolymph of parasitized *L. dispar* larvae. Transcript was detected in hemolymph of parasitized host larvae less than one hour pp (H-30 min) and gene expression remained active for 6 days pp (H-2d, H-4d, H-6d). The level of GiPDV 1.1 expression declined significantly in hemolymph 6 days pp. No detectable GiPDV1.1 expression was observed in hemolymph 8 days pp (H-8d).

expression level in the hemolymph 30 min pp was 191-fold higher than that in the calibrator, brain 6 days pp. Our results suggested that GiPDV 1.1 could be one of those early viral genes expressed rapidly and involved early protection of parasitoid eggs from host immune response. In previous studies, PDV transcripts were not reported to be detected earlier than 2 h pp. Fleming et al. (1983) reported that transcripts of CsV were detected in *H. virescens* larvae 2 h pp. Blissard et al. (1986) detected more than 12 CsPDV transcripts in parasitized *H. virescens* also by 2 h pp. Webb and Luckhart (1996) reported that cellular encapsulation of foreign objects could be very rapid, possibly after as few as 30 min in *H. virescens* as indicated by discrete hemocytes found attached on washed unprotected *C. sonorensis* eggs at 30 min post-egg injection. Although expression of PDV genes was previously detected in the host as early as 2 h pp, it is unclear how the parasitoid eggs escaped encapsulation if cellular immune response began immediately after oviposition. One possibility was that expression level of PDV transcripts was not high enough for Northern detection. The persistence of PDV transcripts in parasitized insects varied significantly. Expression of some PDV viral genes appeared to be highly transient while other viral genes remained at constant levels throughout endoparasite development. Expression of bracovirus genes has been reported

to be transient or decreasing in later stages of parasitization (Asgari et al., 1996; Strand et al., 1997). In both PDV genera, viruses were able to persist without viral replication in parasitized insects to late stages of parasitoid development. The presence of GiPDV 1.1 mRNA through 6 days pp suggested GiPDV 1.1 may have a continuous role in protection of the developing endoparasite. A steep decline in GiPDV 1.1 expression in hemolymph at day 6 pp and disappearance at day 8 pp suggested an association of decline with initiation of later viral gene expression, since host regulation still depended on PDV gene expression.

GiPDV 1.1 expression in the brain of parasitized host larvae was weak compared with expression in the hemolymph. No detectable GiPDV 1.1 transcript was observed at 30 min and 2 days pp. GiPDV 1.1 signal was detected until 4 days pp and the relative expression level in the brain at 4 days pp was 50-fold higher than the calibrator. The predicted GiPDV 1.1 protein sequence had a signal peptide and a cleavage site as well as several potential *N*-glycosylation sites, indicating that GiPDV 1.1 encoded precursor was likely glycosylated and secreted. The temporal GiPDV 1.1 expression in host tissues suggested that GiPDV may first infect host hemocytes, where protein expressed inside PDV-infected hemocytes could function to suppress host immune response. Later the GiPDV 1.1 transcript could have been expressed

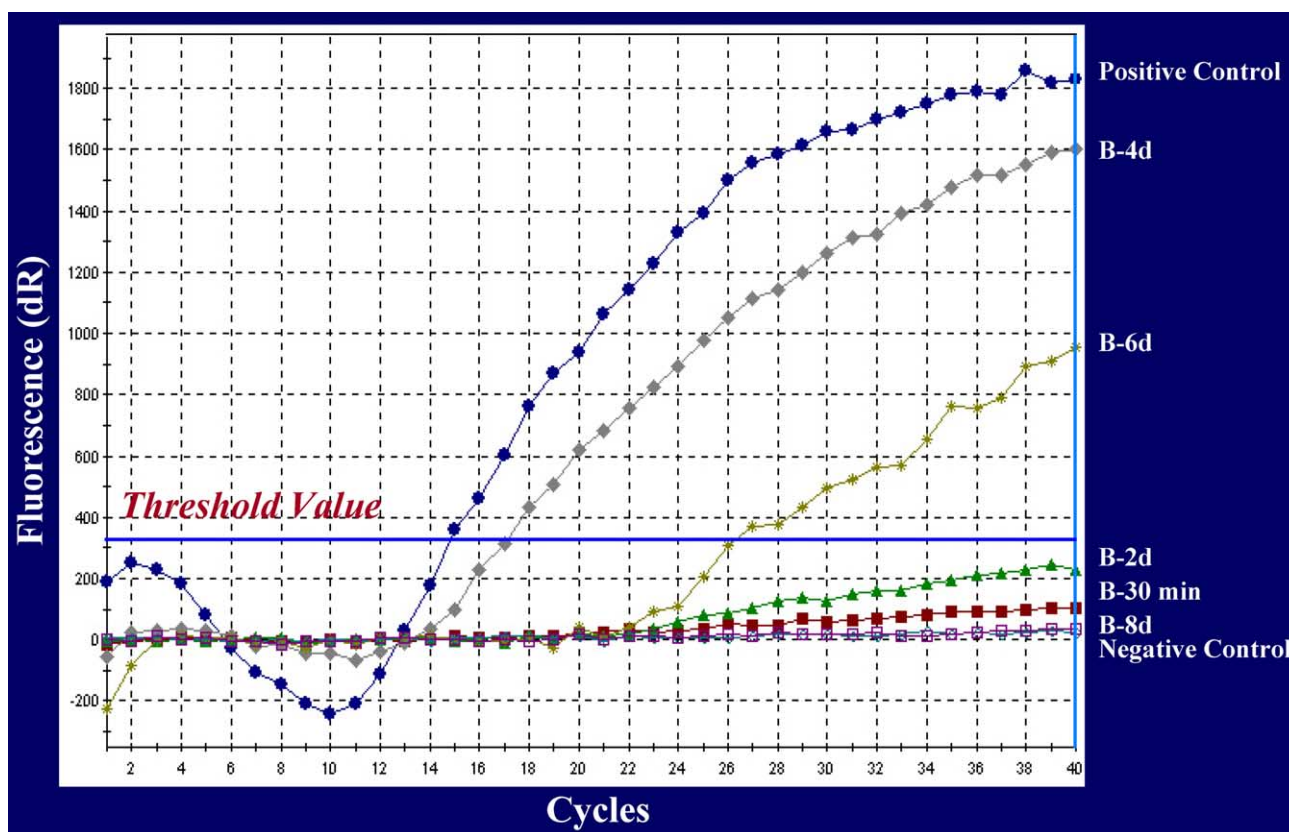


Fig. 5. Representative RT-PCR amplification plot of GiPDV 1.1 expression in brain of *G. indiensis* parasitized *L. dispar* larvae. No GiPDV 1.1 amplification product was detected using template RNA isolated from brain of parasitized larvae at 30 min and 2 days pp (H-30 min, H-2d). GiPDV 1.1 expression was detected in the brain of parasitized larvae 4 days pp (H-4d) and at 6 days pp (H-6d). No detectable GiPDV1.1 expression was observed in brain at 8 days pp (H-8d).

in different tissues, such as brain, to play a potential role in disruption of host immune response or suppression of host development.

The level of viral expression in the host is critical to the virus's ability to suppress host immunity. The higher expression in the host hemolymph, together with abundant expression immediately pp, suggested that the GiPDV 1.1 encoded product may have a role in the abrogation of host cellular immune mechanisms. Webb (1998) suggested that high levels of gene expression may positively correlate with copy number of the viral gene in host tissues, and that success of an endoparasitoid is dependent on the level of PDV gene expression which is entirely dependent on the gene dosage. Our previous studies showed that GiPDV 1.1 gene hybridized to four separate GiPDV genomic segments, two of segments present in higher molar quantity. The multiple hybridization signals of GiPDV 1.1 indicated multiple gene loci within GiPDV and could be caused by homologous sequences or related genes among different GiPDV DNA segments. The ongoing GiPDV genome study in our laboratory will provide information on specific gene homologs among genome segments. The features of genome segmentation, hypermolar segment ratios and sequence homology have been suggested to be involved in increasing the copy number of essential genes and the levels of gene expression in the

absence of virus replication (Xu and Stoltz, 1993; Cui and Webb, 1997). High expression in the parasitized host suggested that high copy numbers of GiPDV 1.1 gene were present in host hemocytes. The variation in temporal and spatial gene expression pp in different host tissues suggested a host regulatory system affects viral expression during parasitism.

Analysis of GiPDV 1.1 gene expression in the parasitized host using real-time quantitative RT-PCR demonstrates that real-time RT-PCR is a rapid, reliable and valid method of potential value for future PDV gene expression studies. Further studies of the GiPDV1.1-encoded protein and its interaction with host proteins may have physiological relevance to understanding host regulatory processes.

References

- Altschul, S.F., Gish, W., Miller, W., Myers, E.W., Lipman, D.J., 1990. Basic local alignment search tool. *J. Mol. Biol.* 215, 403–410.
- Asgari, S., Hellers, M., Schmidt, O., 1996. Host haemocyte inactivation by an insect parasitoid: transient expression of a polydnavirus gene. *J. Gen. Virol.* 77, 2653–2662.
- Bell, R.A., Owens, C.D., Shapiro, M., Tardif, J.R., 1981. Development of mass-rearing technology. In: Donae, C.C., McManus, M.L. (Eds.), *The Gypsy Moth: Research Toward Integrated Pest Management*, pp. 599–633.

- Chen, Y.P., Gundersen-Rindal, D.E., 2003. Morphological and genomic characterization of the polydnavirus associated with the parasitoid wasp, *Glyptapanteles indiensis* (Hymenoptera: Braconidae). J. Gen. Virol. 84, 2051–2060.
- Cui, L., Webb, B.A., 1997. Homologous sequences in the *Campoletis sonorensis* polydnavirus genome are implicated in replication and nesting of the W segment family. J. Virol. 71, 8504–8513.
- Edson, K.M., Vinson, S.B., Stoltz, D.B., Summers, M.D., 1981. Virus in a parasitoid wasp: suppression of the cellular immune response in the parasitoid's host. Science 211, 582–583.
- Fleming, J.G.W., Blissard, G.W., Summers, M.D., Vinson, S.B., 1983. Expression of *Campoletis sonorensis* virus in the parasitized host *Heliothis virescens*. J. Virol. 48, 74–78.
- Lavine, M.D., Beckage, N.E., 1995. Polydnaviruses: potent mediators of host insect immune dysfunction. Parasitol. Today 11, 368–378.
- Lawrence, P.O., Lanzrein, B., 1993. Hormonal interactions between insect endoparasites and their host insects. In: Beckage, N.E., Thompson, S.N., Federici, B.A. (Eds.), Parasites and Pathogens of Insects. Academic Press, New York, pp. 59–86.
- Raeymaekers, L., 1995. A commentary on the practical application of competitive PCR. Genome Res. 5, 91–94.
- Stoltz, D.B., 1993. The polydnavirus life cycle. In: Beckage, N.E., Thompson, S.N., Federici, B.A. (Eds.), Parasites and Pathogens of Insects, vol. 1. Academic Press, New York, pp. 167–187.
- Strand, M.R., Noda, T., 1991. Alterations in the haemocytes of *Pseudoplusia includens* after parasitism by *Microplitis demolitor*. J. Insect Physiol. 37, 839–850.
- Strand, M.R., Wong, E.A., 1991. The growth and role of *Microplitis demolitor* teratocytes in parasitism of *Pseudoplusia includens*. J. Insect Physiol. 37, 503–515.
- Strand, M.R., Witherell, R.A., Trudeau, D., 1997. Two *Microplitis demolitor* polydnavirus mRNAs expressed in hemocytes of *Pseudoplusia includens* contain a common cysteine-rich domain. J. Virol. 71 (3), 2146–2156.
- Webb, B.A., 1998. Polydnavirus biology, genome structure and evolution. In: Miller, L.K., Ball, A. (Eds.), The Insect Viruses. Plenum Press, New York, pp. 105–139.
- Webb, B.A., Luckhart, S., 1996. Factors mediating short- and long-term immune suppression in a parasitized insect. J. Insect Physiol. 42, 33–40.
- Xu, D., Stoltz, D.B., 1993. Polydnavirus genome segment families in the ichneumonid parasitoid *Hyposoter fugitivis*. J. Virol. 67, 1340–1349.